

Kochen-Specker theorem studied with neutron interferometer

Yuji Hasegawa¹, Katharina Durstberger-Rennhofer, Stephan Sponar, and Helmut Rauch

Atominstiut, Technische Universität Wien, Stadionallee 2, A-1020 Wien, Austria

Abstract

The Kochen-Specker theorem theoretically shows evidence of the incompatibility of noncontextual hidden variable theories with quantum mechanics. Quantum contextuality is a more general concept than quantum non-locality which is quite well tested in experiments by using Bell inequalities. Within neutron interferometry we performed an experimental test of the Kochen-Specker theorem with an inequality, which identifies quantum contextuality, by using spin-path entanglement in a single neutron system. Here entanglement is achieved not between different particles, but between degrees of freedom i.e., between spin and path degree of freedom. Appropriate combinations of the spin analysis and the position of the phase shifter allow an experimental verification of the violation of an inequality of the Kochen-Specker theorem. The observed violation $2.291 \pm 0.008 \not\leq 1$ clearly shows that quantum mechanical predictions cannot be reproduced by noncontextual hidden variable theories.

Keywords: neutron interferometer, entanglement, Kochen-Specker theorem, contextuality, degrees of freedom

1. Introduction

It was Einstein, Podolsky, and Rosen (EPR) [1] and afterwards Bell [2] who shed light on the non-local properties between subsystems in quantum mechanics. Separately Kochen and Specker [3] analysed sets of measurements of compatible observables and found the impossibility of their consistent coexistence, i.e., quantum indefiniteness of measurement results. In their scenario, quantum contextuality, a more general concept compared to non-locality, leads to striking phenomena predicted by quantum theory.

Bell inequalities [2] are constraints imposed by local hidden-variable theories (LHVTs) on the values of some specific linear combinations of the averages of the results of spacelike separated experiments on distant systems. Reported experimental violations of Bell inequalities, e.g. with photons [4], neutrons [5] or atoms [6], suggest that quantum mechanics (QM) cannot be reproduced by LHVTs.

While violations of Bell's inequalities due to nonlocal characters of QM is impressive, conflict between measurements on a single-system is another marvelous prediction of QM, as is first stated by Kochen-Specker [3]. Quantum mechanical peculiarity is not limited to space-like separated systems, but found in measurements of a

single nonseparated system: it is important to investigate the consequences of hidden-variable theories for (massive) non-spacelike separated quantum systems, such as neutrons.

LHVTs are a subset of a larger class of hidden-variable theories known as noncontextual hidden-variable theories (NCHVTs). In NCHVTs the result of a measurement of an observable is assumed to be predetermined and not affected by a (previous or simultaneous) suitable measurement of any other compatible or co-measurable observable. It turns out that there exists a conflict between the predictions of QM and NCHVTs which is predicted by the KS theorem [3].

Here, we describe experimental demonstration of the violation in line with the KS theorem by using a massive quantum systems, in particular, two degrees of freedom of single neutrons within a neutron interferometer.

2. Kochen-Specker theorem

The Kochen-Specker (KS) theorem states that there is no contextual hidden variable model possible that reproduces the predictions of QM (for a review see, e.g., Ref. [7]).

The theorem uses two assumptions: (a) value definiteness (all observables defined for a system, e.g. A and B , have predefined values, e.g. $v(A)$ and $v(B)$)

Email address: Hasegawa@ati.ac.at (Yuji Hasegawa)

and (b) noncontextuality (a system possesses a property independently of any measurement context, i.e., independently of how the value is measured). Due to assumption of noncontextuality the relations $v(A+B) = v(A) + v(B)$ and $v(A \cdot B) = v(A) \cdot v(B)$ hold for mutually compatible observables, which have a set of common eigenvectors and thus are together measurable. One can show mathematically that it is impossible to satisfy both relations for arbitrary pairs of compatible operators A and B within QM.

The original proof was given by Kochen and Specker [3] in 1967 which involves 117 vectors in 3 dimensions. Later on simpler proofs were found, e.g., for 9 observables in 4 dimensions (2 spin- $\frac{1}{2}$ particles) by Peres [8] and Mermin [7] who extended Peres' proof into a state independent proof, and with 10 observables in 8 dimensions (3 spin- $\frac{1}{2}$ particles) by Mermin [9] who could also show a connection to the Greenberger-Horne-Zeilinger (GHZ) version [10] of Bells theorem. Up to now the simplest proof of the KS theorem was found by Cabello [11] which uses 18 vectors in 4 dimensions.

We give a short explanation of the proof by Peres and Mermin discussed in Ref. [7]. In 4 dimensions observables are represented by Pauli matrices of two spin- $\frac{1}{2}$ particles σ_i^1 and σ_j^2 where $i, j = \{x, y, z\}$. The square of each matrix is unity, the eigenvalues are ± 1 , in each subspace the normal commutation relations for Pauli operators are satisfied, and the commutator of observables from different subspaces is zero $[\sigma_i^1, \sigma_j^2] = 0$ for any i, j . Consider the following 9 observables A_m arranged in a "magic square":

σ_x^1	σ_x^2	$\sigma_x^1 \cdot \sigma_x^2$	$\rightarrow +1$
σ_y^2	σ_y^1	$\sigma_y^1 \cdot \sigma_y^2$	$\rightarrow +1$
$\sigma_x^1 \sigma_y^2$	$\sigma_y^1 \sigma_x^2$	$\sigma_z^1 \cdot \sigma_z^2$	$\rightarrow +1$
\downarrow	\downarrow	\downarrow	
+1	+1	-1	

In each row and column the observables are mutually commuting and hence compatible. The product of three observables in each row and also in the first two columns is $+1$ but in the last column we get -1 for the product (due to $\sigma_x^k \sigma_y^k = i\sigma_z^k$ for $k = 1, 2$). Thus the product of all rows and columns is -1 . In NCHVTs we assign to each observable a definite value $v(A_m)$. If we take the product over all rows and columns each value $v(A_m)$ appears twice leading to a total product of $+1$. This contradicts the QM predictions.

In contrast to Bell's theorem the KS theorem does not use statistical predictions but relies on logical contradictions. However, in experiments we have finite preces-

sion and thus never perfect correlations which makes it necessary to deduce experimentally testable inequalities from the KS theorem. There are proposals which use the assumptions of contextuality but are not independent from additional QM predictions, e.g. [12], but there are also inequalities which are based only on the assumptions of contextuality [13]. There exist also state-independent inequalities to test KS theorem [14] and the first experiments were done with single photons [15] and ions [16] confirming a violation of the inequality.

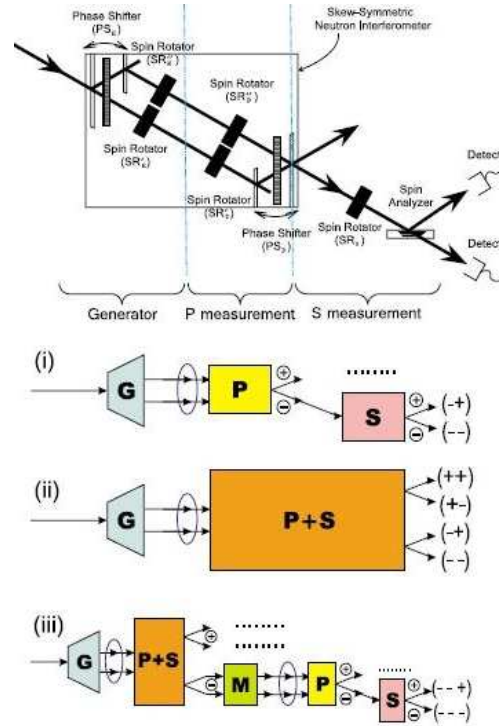


Figure 1: Above: A proposed experimental setup with a neutron interferometer. The interferometer is set in a way that fulfills two functions: the first half works as a state generator, and the second half works as a path measurement apparatus. In both parts, a phase shifter (PS) as well as a pair of spin rotators (SR) are inserted. A spin measurement is carried out on the outgoing beam in the forward direction. Below: Three diagrams for the different measurement "contexts". (i) For measurements of $\sigma_x^s \cdot \sigma_x^p$ and $\sigma_y^s \cdot \sigma_y^p$: After going through a state generator (G), a state suffers a path measurement (P) followed by a spin measurement (S). Consequently, each outgoing beam gives the results of the two measurements. (ii) For measurements of $\sigma_y^s \sigma_x^p \cdot \sigma_x^s \sigma_y^p$: By tuning one of the spin rotators to a spin-flip operation in the path measurement part, the second half of the interferometer together with a spin analyzer (P+S) can discriminate four Bell states, which assign four outgoing beams to the four possible results of the measurements. (iii) For measurements of $\sigma_y^s \sigma_x^p \cdot \sigma_y^s \sigma_x^p$ and $\sigma_x^s \sigma_y^p \cdot \sigma_x^s \sigma_y^p$: After the apparatus P+S, a state mixer (M) eliminates the former information about the result of either observable, and is followed by a path and a spin measurement.

3. Theoretical considerations

With the use of an inequality of the KS theorem [13] one can study the statistical violation of non-contextual assumptions. Exploiting the interference effect of matter waves together with entanglement in a single-particle system, neutron interferometric experiments [17] are suitable to exhibit phenomena associated with the KS theorem. At the first stage of experimental tests of quantum contextuality, we carried out interferometric experiments demonstrating Kochen-Specker-like phenomena [18]. Further theoretical analysis revealed a more advanced scheme based on the Peres-Mermin proof of the KS theorem and an experiment with neutron interferometry was proposed [13]. Here, an improved experimental test of the KS theorem using single neutrons is described where the entanglement occurs between two degrees of freedom in a single-system [19].

For the proof of the KS theorem, we consider single neutrons prepared in a maximally entangled Bell-like state

$$|\Psi_n^{Bell}\rangle = \frac{1}{\sqrt{2}}(|\downarrow\rangle \otimes |I\rangle - |\uparrow\rangle \otimes |II\rangle), \quad (1)$$

where $|\uparrow\rangle$ and $|\downarrow\rangle$ denote spin-up and spin-down eigenstates of the neutron, and $|I\rangle$ and $|II\rangle$ denote the two beam paths in the neutron interferometer [5]. The proof is based on six observables σ_x^s , σ_x^p , σ_y^s , σ_y^p , $\sigma_x^s\sigma_y^p$ and $\sigma_y^s\sigma_x^p$, where the superscripts s and p indicate the spin and path degree of freedom, respectively, and the following five quantum mechanical predictions for the Bell-like state $|\Psi_n^{Bell}\rangle$

$$\sigma_x^s \cdot \sigma_x^p |\Psi_n^{Bell}\rangle = -|\Psi_n^{Bell}\rangle, \quad (2a)$$

$$\sigma_y^s \cdot \sigma_y^p |\Psi_n^{Bell}\rangle = -|\Psi_n^{Bell}\rangle, \quad (2b)$$

$$\sigma_x^s\sigma_y^p \cdot \sigma_x^s \cdot \sigma_y^p |\Psi_n^{Bell}\rangle = +|\Psi_n^{Bell}\rangle, \quad (2c)$$

$$\sigma_y^s\sigma_x^p \cdot \sigma_y^s \cdot \sigma_x^p |\Psi_n^{Bell}\rangle = +|\Psi_n^{Bell}\rangle, \quad (2d)$$

$$\sigma_x^s\sigma_y^p \cdot \sigma_y^s\sigma_x^p |\Psi_n^{Bell}\rangle = -|\Psi_n^{Bell}\rangle. \quad (2e)$$

The inconsistency arising in any attempt to ascribe the predefined values -1 or $+1$ to each and every of the six observables can be easily seen by multiplying Eqs. (2a)-(2e). Since each observable appears twice, the left hand sides give $+1$ while the product of the right hand sides is -1 .

Since no experiment can show perfect correlations or anti-correlations, one needs an experimentally testable inequality: this can be derived from the linear combination of the five expectation values with the respective quantum mechanical predictions as linear coefficients.

It can be shown that in any NCHVT

$$-\langle \sigma_x^s \cdot \sigma_x^p \rangle - \langle \sigma_y^s \cdot \sigma_y^p \rangle + \langle \sigma_x^s \sigma_y^p \cdot \sigma_x^s \cdot \sigma_y^p \rangle + \langle \sigma_y^s \sigma_x^p \cdot \sigma_y^s \cdot \sigma_x^p \rangle - \langle \sigma_x^s \sigma_y^p \cdot \sigma_y^s \sigma_x^p \rangle \leq 3, \quad (3)$$

in contrast to the prediction of 5 by QM. While Eqs. (2a)-(2b) and (2e) represent state dependent predictions relying on the specific properties of the neutron's Bell-like state $|\Psi_n^{Bell}\rangle$, Eqs. (2c)-(2d) are state-independent predictions which hold in any NCHVT. In other words, in any NCHVT, $\langle \sigma_x^s \sigma_y^p \cdot \sigma_x^s \cdot \sigma_y^p \rangle = 1$ and $\langle \sigma_y^s \sigma_x^p \cdot \sigma_y^s \cdot \sigma_x^p \rangle = 1$. Therefore, any NCHVT must satisfy not only inequality (3), but also the following inequality in a reduced form:

$$-\langle \sigma_x^s \cdot \sigma_x^p \rangle - \langle \sigma_y^s \cdot \sigma_y^p \rangle - \langle \sigma_x^s \sigma_y^p \cdot \sigma_y^s \sigma_x^p \rangle \leq 1. \quad (4)$$

A violation of inequality (4) in an experiment reveals quantum contextuality.

4. Neutron interferometric experiments

The experiment was carried out at the neutron interferometer instrument S18 at the high-flux reactor of the Institute Laue-Langevin (ILL) in Grenoble, France. The setup of the experiment is depicted in Fig.2. A monochromatic beam, with mean wavelength $\lambda_0 = 1.92$ ($\Delta\lambda/\lambda_0 \sim 0.02$) and 5×5 mm² beam cross-section, is polarized by a bi-refracting magnetic field prism in \hat{z} -direction. Due to the angular separation at the deflection, the interferometer is adjusted so that only the spin-up component fulfills the Bragg condition at the first interferometer plate (beam splitter). Behind the beam splitter the neutrons wave function is found in a coherent superposition of path $|I\rangle$ and $|II\rangle$. Together with a radio-frequency (RF) spin-flipper in path $|I\rangle$, denoted as RF_{ω}^I , the first half of the interferometer is used for the generation of the maximally entangled Bell-like state, Eq. (1). In this experiment, RF spin-flippers are used for the spin-flips to avoid unwanted contrast reduction due to dephasing effect by the Mu-metal, used in the previous experiment [18]. Apart from the RF flipper in path $|I\rangle$ our experiment requires a second RF flipper in the interferometer (RF_{ω}^{II}) and another RF flipper in the O-beam (in the forward direction) operated at half frequency ($RF_{\omega/2}$).

The first term in inequality (4) requires the measurement of σ_x^s together with σ_x^p . Here, $RF_{\omega/2}$ in the O-beam is needed for compensating the energy difference due to the spin flip at RF_{ω}^I [20], while the second RF flipper in the interferometer, RF_{ω}^{II} , is turned off. For measuring the path observable, i.e. σ_x^p , the phase

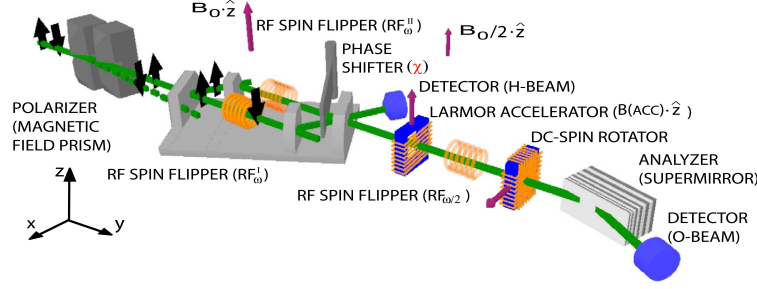


Figure 2: Experimental setup for studying Kochen-Specker theorem based on the Peres-Mermin proof with neutron interferometer. The RF flipper in the path I (RF_{ω}^I) generates the Bell-like state $|\Psi_n^{Bell}\rangle$. By turning either the RF flipper in the path II (RF_{ω}^{II}) or another RF flipper ($RF_{\omega/2}$) on, together with suitable spin analysis, intensity oscillations are obtained in phase shifter χ scans. From the data on the appropriate settings, expectation values of the measurements $\sigma_x^s \cdot \sigma_x^p$, $\sigma_y^s \cdot \sigma_y^p$, and $\sigma_x^s \sigma_y^p \cdot \sigma_y^s \sigma_x^p$ are determined.

shifter is adjusted to $\chi = 0$ and $\chi = \pi$ in the path state $|\Psi(\chi)\rangle_p = \frac{1}{\sqrt{2}}(|I\rangle + e^{i\chi}|II\rangle)$, which correspond to the projections to $|+x\rangle_p$ and $|-x\rangle_p$, the two eigenstates of σ_x^p , respectively. The spin analysis in the $x-y$ plane is accomplished by the combination of the Larmor accelerator DC coil inducing a Larmor phase $\alpha = 0$ and $\alpha = \pi$, a $\pi/2$ DC spin-rotator and an analyzing supermirror. This configuration allows projective measurements along $|+x\rangle_s$ and $|-x\rangle_s$ direction, the two eigenstates of σ_x^s .

The experimental setup for the second term in inequality (4) is identical with the one for the first term, but the measurement of σ_y^s together with σ_y^p is achieved with the settings $\chi = \frac{\pi}{2}, \frac{3\pi}{2}$ and $\alpha = \frac{\pi}{2}, \frac{3\pi}{2}$. Typical intensity oscillations for the successive measurement of the path and the spin component are shown in Fig. 3 top. The expectation values are experimentally determined from the count rates

$$E(\alpha, \chi) = \frac{N(\alpha, \chi) + N(\alpha + \pi, \chi + \pi) - N(\alpha + \pi, \chi) - N(\alpha, \chi + \pi)}{N(\alpha, \chi) + N(\alpha + \pi, \chi + \pi) + N(\alpha + \pi, \chi) + N(\alpha, \chi + \pi)}, \quad (5)$$

where $N(\alpha, \chi)$ denotes the count rate for the joint measurement of spin and path. The required count rates at appropriate settings of α and χ are extracted from least squares fits in Fig. 3 top, indicated by the vertical dashed lines. From these intensities the expectation values were determined as $\langle \sigma_x^s \cdot \sigma_x^p \rangle \equiv E(0, 0) = -0.679 \pm 0.005$ and $\langle \sigma_y^s \cdot \sigma_y^p \rangle \equiv E(\frac{\pi}{2}, \frac{\pi}{2}) = -0.682 \pm 0.005$.

The third term in inequality (4) requires the measurement of $\sigma_x^s \sigma_y^p$ together with $\sigma_y^s \sigma_x^p$. Measuring the product of these two observables simultaneously implies the discrimination of the four possible outcomes $(\sigma_x^s \sigma_y^p, \sigma_y^s \sigma_x^p) = \{(+1, +1), (-1, -1), (+1, -1), (-1, +1)\}$, which is equivalent to a complete Bell-state discrimination. The two operators $\sigma_x^s \sigma_y^p$ and $\sigma_y^s \sigma_x^p$ have the four common

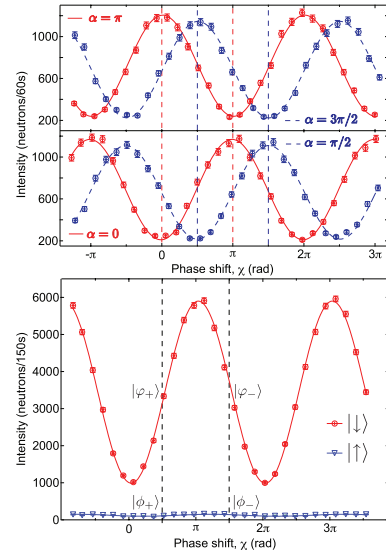


Figure 3: Typical intensity modulations obtained by varying the phase χ for the path subspace. The spin analysis of $\pm x$ - and $\pm y$ -directions were involved (top). Another spin-flipper in the interferometer was turned on and the spin analysis of $\pm z$ -directions were carried out (bottom).

Bell-like eigenstates

$$|\varphi_{\pm}\rangle = \frac{1}{\sqrt{2}}(|\downarrow\rangle \otimes |I\rangle \pm i|\uparrow\rangle \otimes |II\rangle), \quad (6a)$$

$$|\phi_{\pm}\rangle = \frac{1}{\sqrt{2}}(|\uparrow\rangle \otimes |I\rangle \pm i|\downarrow\rangle \otimes |II\rangle), \quad (6b)$$

with the corresponding eigenvalue equations

$$\sigma_x^s \sigma_y^p |\varphi_{\pm}\rangle = \pm |\varphi_{\pm}\rangle, \quad \sigma_y^s \sigma_x^p |\varphi_{\pm}\rangle = \mp |\varphi_{\pm}\rangle, \quad (7a)$$

$$\sigma_x^s \sigma_y^p |\phi_{\pm}\rangle = \pm |\phi_{\pm}\rangle, \quad \sigma_y^s \sigma_x^p |\phi_{\pm}\rangle = \pm |\phi_{\pm}\rangle. \quad (7b)$$

It follows that the outcome -1 for the product measurement of $\sigma_x^s \sigma_y^p$ and $\sigma_y^s \sigma_x^p$ is obtained for $|\varphi_{\pm}\rangle$, while

the states $|\phi_{\pm}\rangle$ yield the result $+1$. In practice, this Bell-state discrimination is accomplished by the second RF flipper in the interferometer i.e. transforming the state $|\Psi\rangle \rightarrow \frac{1}{\sqrt{2}}(|\downarrow\rangle \otimes |I\rangle - |\downarrow\rangle \otimes |II\rangle)$. When the DC spin-rotator in the O-beam is adjusted to induce a π -flip, only $|\downarrow\rangle$ -spin components reach the detector. Inducing a relative phase χ between the two beam paths in the interferometer allows then for projections to the state $|\phi(\chi)\rangle = \frac{1}{\sqrt{2}}(|\downarrow\rangle \otimes |I\rangle + e^{i\chi} |\uparrow\rangle \otimes |II\rangle)$. According to the definition of $|\phi_{\pm}\rangle$, given in Eq.(6a), phase settings of $\chi = \pm\frac{\pi}{2}$ correspond to the measurement of $|\phi_{\pm}\rangle$. The $|\uparrow\rangle$ -spin analysis is achieved by switching the DC spin-rotator off, where neutrons in the state $|\phi(\chi)\rangle = \frac{1}{\sqrt{2}}(|\uparrow\rangle \otimes |I\rangle + e^{i\chi} |\downarrow\rangle \otimes |II\rangle)$ can be selected, yielding a $|\phi_{\pm}\rangle$ measurement for $\chi = \pm\frac{\pi}{2}$. By rotating the phase shifter, clear sinusoidal intensity oscillation and a low-intensity fluctuation were observed, which is depicted in Fig.3 bottom. The expectation value $\langle\sigma_x^s \sigma_y^p \cdot \sigma_y^s \sigma_x^p\rangle$ is derived using the relation

$$E' = \frac{N'(\phi_+) + N'(\phi_-) - N'(\phi_+) - N'(\phi_-)}{N'(\phi_+) + N'(\phi_-) + N'(\phi_+) + N'(\phi_-)}, \quad (8)$$

where N' denotes the neutron count rate at the desired projections. As done before, least square fits were applied to deduce the count rates at the four projections. From the intensities on the dashed lines in the figure, we obtained the value $\langle\sigma_x^s \sigma_y^p \cdot \sigma_y^s \sigma_x^p\rangle \equiv E' = -0.93 \pm 0.003$. The observed intensities reflect the quantum mechanical predictions for the measurement of the four Bell-like states given by the expectation values $\langle\Psi|\phi_{\pm}\rangle\langle\phi_{\pm}|\Psi\rangle = \frac{1}{2}$ and $\langle\Psi|\phi_{\pm}\rangle\langle\phi_{\pm}|\Psi\rangle = 0$.

With the three experimentally derived expectation values we can finally test inequality (4). We obtain $-\langle\sigma_x^s \cdot \sigma_x^p\rangle - \langle\sigma_y^s \cdot \sigma_y^p\rangle - \langle\sigma_x^s \sigma_y^p \cdot \sigma_y^s \sigma_x^p\rangle = 2.291 \pm 0.008 \not\leq 1$. This clearly confirms the conflict with NCHVTs.

5. Concluding remarks

Neutron interferometric investigations on the KS theorem is described. Entanglement between degrees of freedom in a single-neutron system is exploited: a Bell-like state comprising spin-path entanglement is generated. The proof is based on the Peres-Mermin criteria. An inequality was derived for the evaluation of the experimental data. Expectation values of three different contexts are determined: the final results clearly exhibit the conflict between NCHVTs and QM. It is worth mentioning that the conflict of the KS theorem is not due to the entanglement but can be assigned to the structure of observables: quantum observables have a particular

structure which is different from that of classical observables. We now proceed further studies of quantum contextuality with the use of triply entangled (spin-path-energy entangled) states in a single-neutron system. In addition, neutron polarimeter experiments are used for similar studies, where tunable multi energy levels in addition to spin can be manipulated with very high efficiency.

Acknowledgements

We thank all colleagues who were involved in carrying out experiments presented here; in particular, we appreciate G. Badurek, H. Bartosik, A. Cabello, S. Filipp, D. Home, J. Klepp, R. Loidl, and C. Schmitzer. This work has been supported partly by the Austrian Fonds zur Förderung der Wissenschaftlichen Forschung (FWF), No. P21193-N20 and Hertha-Firnberg-Programm T389-N16.

- [1] A. Einstein, B. Podolsky, and N. Rosen, Phys. Rev. **47**, 777 (1935).
- [2] J. S. Bell, Physics **1**, 195 (1964).
- [3] S. Kochen and E.P. Specker, J. Math. Mech. **17**, 59 (1967).
- [4] G. Weihs, T. Jennewein, C. Simon, H. Weinfurter, and A. Zeilinger, Phys. Rev. Lett. **81**, 5039 (1998).
- [5] Y. Hasegawa, R. Loidl, G. Badurek, M. Baron, and H. Rauch, Nature (London) **425**, 45 (2003).
- [6] D. N. Matsukevich, P. Maunz, D. L. Moehring, S. Olmschenk, and C. Monroe, Phys. Rev. Lett. **100**, 150404 (2008).
- [7] N.D. Mermin, Rev. Mod. Phys. **65**, 803 (1993).
- [8] A. Peres, Phys. Lett. A **151**, 107 (1990).
- [9] D. Mermin, Phys. Rev. Lett. **65**, 3373 (1990).
- [10] D.M. Greenberger, M.A. Horne, A. Zeilinger, in M. Kafatos(Ed.), Bell's Theorem, Quantum Theory, and Conceptions of the Universe, Kluwer Academic, Dordrecht, (1989).
- [11] A. Cabello, J.M. Esteban, and G. García-Alcaine, Phys. Lett. A **212**, 183 (1996).
- [12] C. Simon, C. Brukner, and A. Zeilinger, Phys. Rev. Lett. **86**, 4427 (2001).
- [13] A. Cabello, S. Filipp, H. Rauch, and Y. Hasegawa, Phys. Rev. Lett. **100**, 130404 (2008).
- [14] A. Cabello, Phys. Rev. Lett. **101**, 210401 (2008).
- [15] E. Amsellem, M. Radmark, M. Bourennane, and A. Cabello, Phys. Rev. Lett. **103**, 160405 (2009).
- [16] G. Kirchmair, F. Zähringer, R. Gerritsma, M. Kleinmann, O. Gühne, A. Cabello, R. Blatt, and C. F. Roos, Nature (London) **460**, 494 (2009).
- [17] H. Rauch and S.A. Werner, Neutron interferometry, Clarendon Press, Oxford (2000).
- [18] Y. Hasegawa, R. Loidl, G. Badurek, M. Baron, and H. Rauch, Phys. Rev. Lett. **97**, 230401 (2006).
- [19] H. Bartosik, J. Klepp, C. Schmitzer, S. Sponar, A. Cabello, H. Rauch, and Y. Hasegawa, Phys. Rev. Lett. **103**, 040403 (2009).
- [20] S. Sponar, J. Klepp, R. Loidl, S. Filipp, G. Badurek, Y. Hasegawa, and H. Rauch Phys. Rev. A **78**, 061604(R) (2008).